Reports

Structure of Ice VI

Abstract. *Ice VI, a high-pressure form of density 1.31 g cm^{-3}, has a tetragonal cell of dimensions* a = *6.27 Å,* c = *5.79 Å, space group* P4_2/nmc, *each cell containing ten water molecules. The structure is built up of hydrogen-bonded chains of water molecules that are analogs of the tectosilicate chains out of which the fibrous zeolites are constructed. The chains in ice VI are linked laterally to one another to form an open, zeolite-like framework. The cavities in this framework are filled with a second framework identical with the first. The two frameworks interpenetrate but do not interconnect, and the complete structure can thus be considered a "self-clathrate." This structural feature is a natural way to achieve high density in tetrahedrally linked framework structures.*

The stability conditions of the known forms of ice (Fig. 1) are a reflection of the thermodynamic relations among the various phases, and these relations are in turn a macroscopic reflection of the molecular architecture of the individual forms. Conversely, the structural features of the individual forms in relation to their stability fields and to the thermodynamic variables provide some insight into the forces of interaction between water molecules, and in particular into the disruption of these forces that is caused by packing the molecules more closely together, as is achieved under high pressure. Some structural information for most of the forms of ice is now available (Table 1), and the detailed structures of ice I, Ic, II, III, and VII are known (*1–5*). I here describe the structure of ice VI, determined by x-ray diffraction, and give preliminary x-ray structural information for ice V (Table 1).

The samples were prepared as follows. Short glass capillaries, filled with water, were placed in a hollow steel cylinder fitted with pistons at both ends. The chamber thus formed was filled with gasoline, to transmit pressure from the pistons to the water samples. By loading the pistons and controlling the cylinder temperature appropriately (Fig. 1), the desired ice phase can be formed. The sample is then quenched by immersing the cylinder in liquid nitrogen, the pressure is released, and the sample is forced out of the cylinder and into a bath of liquid nitrogen. At the temperature of liquid nitrogen (−196°C), high-pressure ice samples are metastable and can be kept indefinitely at atmospheric pressure. When the capillaries are removed into the open air, they explode, because of the volume increase upon inversion of the high-pressure ice to ordinary ice I.

Individual capillaries were mounted for x-ray study in a precession camera, where they were maintained at a temperature of −175°C by a stream of cooled nitrogen gas. The precession camera can be used to obtain x-ray powder data, to search the capillaries for crystals suitable for single-crystal study, and to orient and collect complete diffraction data from such crystals.

Ice VI, prepared and examined in this way, gives a powder pattern (Table 2) in general agreement with data obtained at high pressure and also with data from other experiments on quenched samples (*6*). Single crystals are easily obtained and are found to be tetragonal with unit cell dimensions $a = 6.27 \pm 0.01$ Å, $c = 5.79 \pm 0.01$ Å. The diffraction patterns show extinctions for reflections of type $hk0$ with $h + k$ odd and for hhl with l odd. The space group is thus uniquely determined as $P4_2/nmc$ (*7*). The foregoing cell accounts well for the observed powder spacings (Table 2).

Recently single crystal data for ice VI, obtained at high pressure by means of a pressure cell mounted on a precession camera, have been published by Block, Weir, and Piermarini (*8*). These authors report an orthorhombic cell with dimensions $a' = 8.38$ Å, $b' = 6.17$ Å, and $c' = 8.90$ Å, and for this cell they report diffraction extinctions for reflections of type $h'k'0$ with h' odd (diffraction aspect $P \cdot \cdot a$). This identification of the unit cell is erroneous. The cell chosen by Block *et al.* (*8*) is related to the true tetragonal cell as follows. The b' axis is one of the tetragonal a-axes, and the a' axis is the tetragonal cell diagonal [101], that is, $\mathbf{a}' = \mathbf{a} + \mathbf{c}$. The c' axis chosen by Block *et al.* (*8*) should evidently correspond to the other cell diagonal [10$\bar{1}$]. The angle between the a' and c' axes is 94.5°, according to the dimensions of the tetragonal cell, rather than 90° as apparently assumed by Block *et al.* (*8*).

Table 1. X-ray structural data for ice polymorphs.

Ice	Density* (g cm^{-3})	Crystal system	Space group	Cell dimensions (Å)*	Z†	Reference
I	0.92	Hexagonal	$P6_3/mmc$	a 4.48, c 7.31	4	(*1*)
Ic	0.92	Cubic	$Fd3m$	a 6.35	8	(*2*)
II	1.17	Rhombohedral	$R\bar{3}$	a 7.78, α 113.1°	12	(*3*)
III	1.14	Tetragonal	$P4_12_12$	a 6.79, c 6.79	12	(*4*)
IV	1.28					(*14*)
V	1.23	Monoclinic	$A2/a$	a 9.22, b 7.54 c 1035, β 109.2°	28	‡
VI	1.31	Tetragonal	$P4_2/nmc$	a 6.27, c 5.79	10	‡
VII	1.50	Cubic	$Pn3m$	a 3.41	2	(*5*)

* At atmospheric pressure and −175°C. † Number of molecules in the unit cell. ‡ Data given in accompanying text.

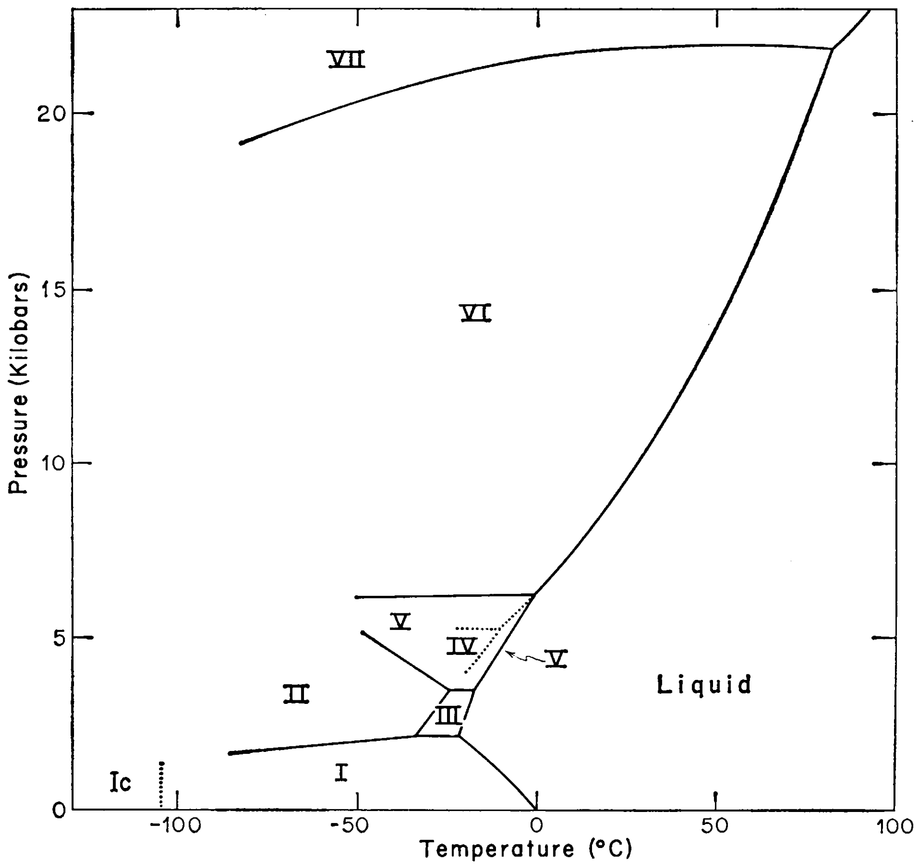

Fig. 1. Phase diagram for water. The solid phases (ice polymorphs) are identified by the roman numeral designations assigned by Bridgman (*14, 9, 15*), upon whose data the diagram is based. The field of ice IV in relation to ice VI and liquid is plotted by dotted lines within the ice V field, and is plotted by analogy to D_2O ice, for which the field was actually measured (*14*); ice IV is everywhere unstable relative to ice V. Ice Ic ("cubic ice") is shown schematically below the temperature of about −105°C, below which it forms by vapor condensation (*16*) and above which it inverts to ice I (*17*); it is not known to have a field of actual stability.

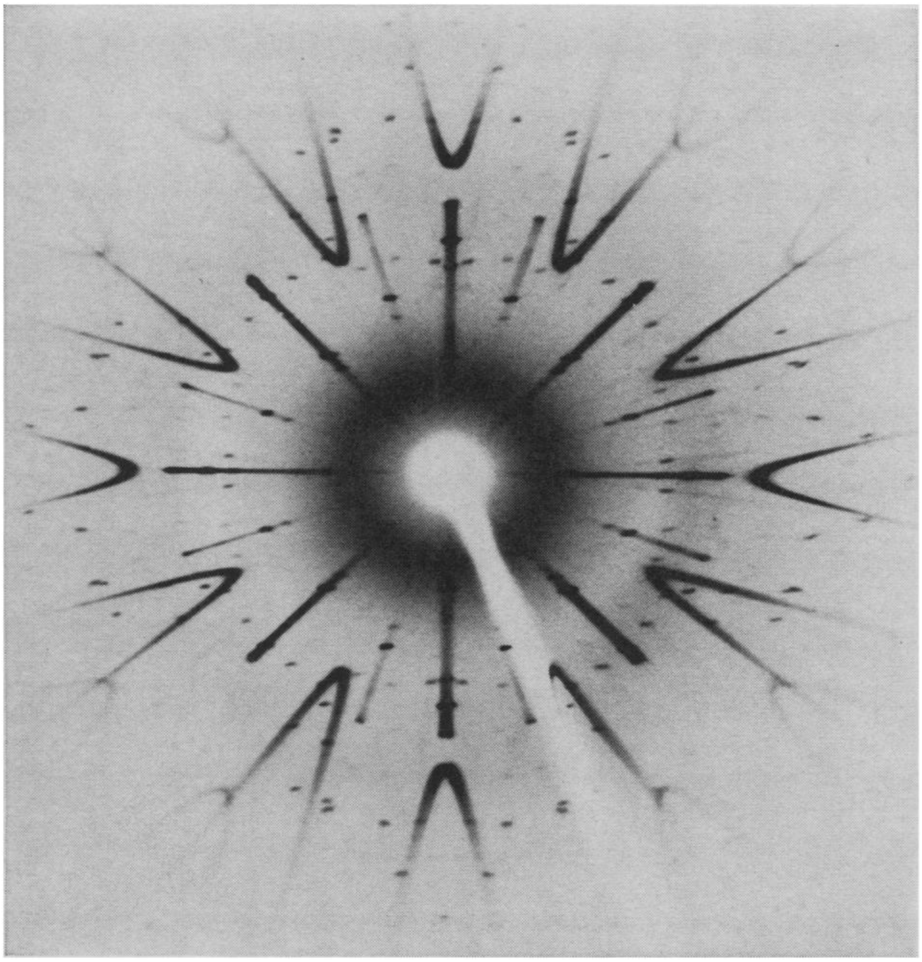

Fig. 2. Precession photograph about the *c*-axis of ice VI, made with unfiltered molybdenum radiation and without a layer-line screen, $\mu = 15°$. The *hk*0 plane shows as single spots in the central portion of the photograph, *hk*1 and higher layers as double spots and hyperbolic streaks in the outer portion. Note 4-fold symmetry about the *c*-axis.

Proof of the correct unit cell is essential to determination of the structure; hence in Fig. 2 there is shown a precession photograph of the *hk*0 plane of ice VI. The photograph was made without use of a layer-line screen and hence shows also the symmetry of the upper layers parallel to *hk*0. It is thus analogous to a Laue photograph in exhibiting the diffraction symmetry of the crystal about its *c*-axis. The 4-fold axis and the mirror planes are clearly visible. There are no 4-fold axes parallel to the plane of the photograph. Their absence cannot be judged from the photograph itself, but is determined by manipulating the original crystals.

It is unlikely that the crystals studied by Block *et al.* (*8*) at high pressure were essentially different from the quenched samples of ice VI described here. The unit cell chosen by these authors is compatible with essentially the same powder pattern as is given by the quenched samples (Table 2), and the dimensions of the "orthorhombic" and tetragonal cells are compatible, taking into account the differing cell orientations and the different experimental conditions and possible sources of experimental error. The *h'k'*0 photograph published by Block *et al.* (Fig. 1 of Ref. *8*) appears identical, to the extent that the diffraction pattern can be seen in the photograph, with precession photographs of the *hkh* plane of the tetragonal crystals. The two crystals (ice VI under pressure, and quenched) can therefore differ at most by a slight distortion. It is unlikely that a low-temperature (quenched) form would be more symmetrical (tetragonal) than the high-temperature form (supposedly orthorhombic) from which it inverted by a displacive transformation upon cooling.

The density of ice VI at 6175 atmospheres and 0.2°C (the triple point ice V–ice VI–liquid) is 1.33 g cm^{-3} (*9*). If the compressibility measured over the range 6175 to 8710 atm (*9*) holds over the range from 6175 atm down to 0, the density at zero pressure would be 1.31 g cm^{-3}. This density and the cell dimensions imply that the unit cell of ice VI contains ten water molecules (calculated density 1.314 g cm^{-3}). These ten molecules must be located at special positions in space group $P4_2/nmc$, since the general position in this space group has 16-fold multiplicity (*7*). The particular special positions occupied can be deduced by a process of elimination based on the chemical expectation that no two water molecules will be closer than about 2.7 Å. This condition leads to a unique solution for the structure of ice VI. Eight of the oxygen atoms of the water molecules occupy position 8 *g*, having coordinates of the form 0, *x*, *z* with $x = 0.276$, $z = 0.382$, and the remaining two oxygen atoms occupy position 2 *a*, at 0, 0, 0 and 1/2, 1/2, 1/2. The values of *x* and *z* given are chosen so as to make the distances from each oxygen atom to its four nearest neighbors equal.

The structure so derived is tested by comparing structure factors calculated from it with structure factors determined from the intensities of x-ray reflections from ice VI. For this purpose reflections of type *h0l*, obtained from precession photographs of this plane, are sufficient since a tetragonal structure is completely defined in *a*-axis projection. The comparison (Table 3) shows agreement so close as to verify that the structure is correct in detail. The parameter values *x* and *z* given must be accurate (probably to ± 0.002), since the "fractional discrepancy" $\Sigma|\Delta F|/\Sigma|F_0|$ is only 0.07, which is about as low as is commonly achieved for refined structures based on photographically measured x-ray intensities.

Positions of the hydrogen atoms cannot be closely defined from the x-ray diffraction data because hydrogen atoms scatter x-rays only weakly. The hydrogen atoms doubtless lie somewhere near the line of centers between oxygen atoms hydrogen-bonded to one another.

The structure of ice VI is plotted in *c*-axis projection in Fig. 3 and is drawn in Fig. 4 in such a way as to bring out its component parts. Each water molecule (the oxygen atom of which is represented by a ball in Figs. 3 and 4) has four nearest neighbors at a distance of 2.81 Å, and is evidently hydrogen-bonded to these. The four neighbors form a rather highly distorted tetrahedron around the central water molecule. The water molecules are linked together by the hydrogen bonds (shown as sticks in Figs. 3 and 4) to form chains parallel to the *c*-axis of the crystal (column A, Fig. 4). The chains link sideways to one another, parallel to the crystal

Table 2. X-ray powder data for ice VI.

*I**	d_{obs}* (Å)	d_{obs}*† (Å)	d_{calc}‡ (Å)	*hkl*
		4.44	4.47	110
8*h*	4.3	4.27	4.26	101
8*h*	3.6			
5*h*	3.4			
13	3.12	3.14	3.14	200
8	2.91	2.92	2.90	002
90	2.75	2.76	2.76	201
50	2.63	2.64	2.63	102
100	2.51	2.53	2.52	211
8	2.43	2.43	2.42	112
25	2.21	2.22	2.21	220
13*b*	2.10		2.13	202
20	2.01	2.02	2.01	212
20	1.97	1.98	1.98	310
17*b*	1.85	1.85	1.85	103
1*b*	1.75		1.75	222
25*b*	1.64		1.66	321
			1.64	203
			1.64	312
20	1.56		1.57	400
25	1.48		1.49	322
			1.48	330
3	1.44		1.45	004
12	1.41		1.42	303
7*b*	1.37		1.38	402
			1.38	313
			1.38	114
			1.36	421
			1.35	412

* Intensity values (*I*) and observed spacings (*d*, in Å) from quenched samples reported by Bertie, Calvert, and Whalley (*6*); *h* indicates lines in region masked by diffraction halo from silica glass tube; *b* designates broad lines. † Spacings (Å) measured from powder patterns in present work. Listing is incomplete because no attempt was made to measure the complete pattern. Relative intensities agree with those reported in column 1, with the exception of lines reported at 3.6 and 3.4 Å, which are missing. ‡ Calculated spacing (d_{calc}) from unit cell given in text.

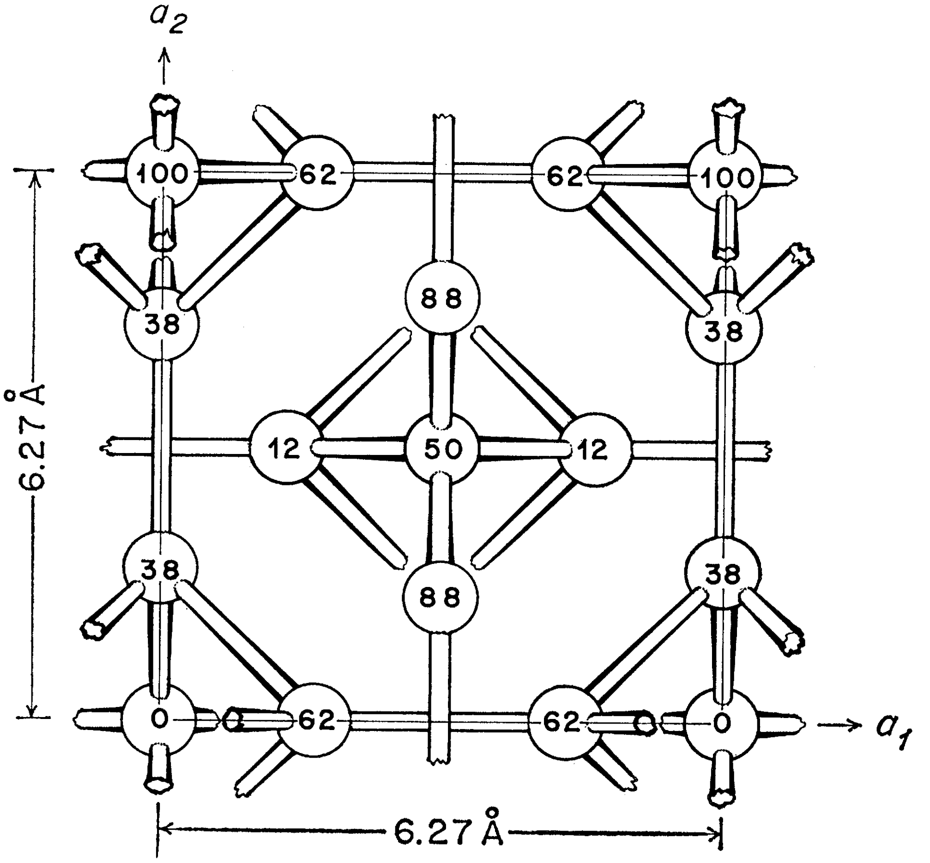

Fig. 3. Structure of ice VI, viewed along the *c*-axis of the crystal. Oxygen atoms of the water molecules are shown as balls, and hydrogen bonds linking the molecules are represented by sticks. Hydrogen atoms are not shown. Heights of the atoms above the plane of projection are marked in hundredths of the *c*-axial length (5.79 Å). Note the two hydrogen-bonded frameworks that interpenetrate but do not interconnect. The chains depicted in Fig. 4, column A, upper line, run toward the viewer through the corners of the cell, and those in column A, lower line, run through the center of the cell.

a-axes, so as to build a complete framework of parallel chains linked together (column B, Fig. 4). This framework is a rather open one, and there are large cavities among the chains. The cavities are of such size and shape that two complete frameworks, related by a 90° rotation (4_2 axis), can be combined together to make the complete structure (column C, Fig. 4). The cavities of one framework accommodate the chains of the second framework, and the cavities of the second accommodate the chains of the first.

An individual hydrogen-bonded framework (column B), with its interstitial cavities, can be likened to the ice-like frameworks that occur in clathrate hydrates (*10*). In clathrate hydrates the cavities commonly accommodate organic or noble gas molecules. In ice VI, however, the cavities of one framework accommodate a second framework identical with the first; hence the crystal is in a sense a "self-clathrate." A similar situation occurs in ice VII, which is likewise built of two interpenetrating but noninterbonded frameworks (*5*). In ice VII the two frameworks are not sharply distinguished from one another, owing to the fact that the four inter-framework contacts made by each water molecule are just as short as the four hydrogen bonds (intra-framework linkages) made by it. Ice VI contrasts in that the inter-framework contacts are all considerably

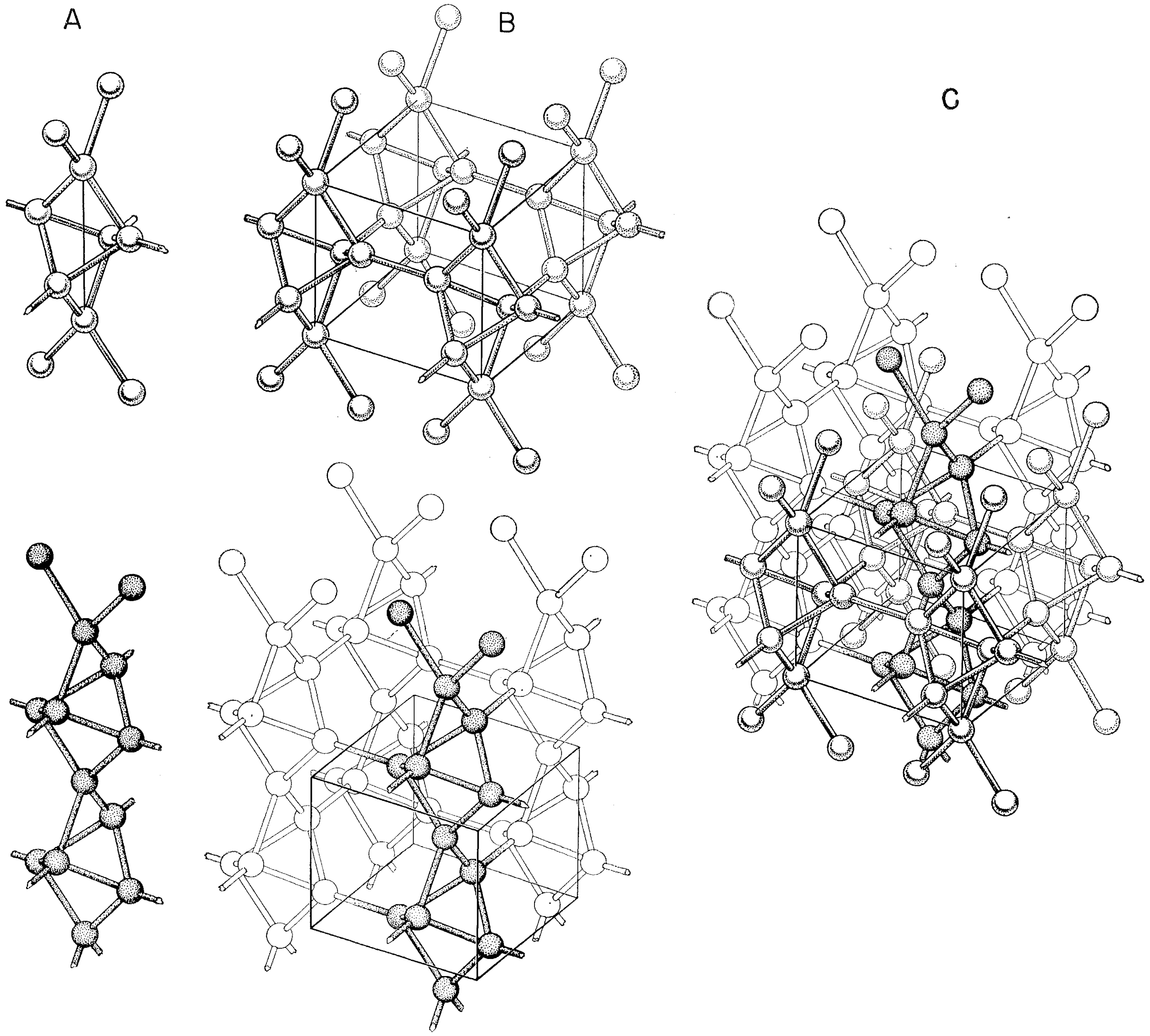

Fig. 4. Structure of ice VI, shown by assembly of its component parts. In column A are shown hydrogen-bonded chains of water molecules running parallel to the *c*-axis of the crystal. The chain below is identical with the one above but is rotated through 90°. Oxygen atoms of water molecules are represented by balls, and hydrogen bonds by sticks; the hydrogen atoms are not shown. In column B such chains are linked sideways to form two framework structures and are placed in their proper location relative to the unit cell (outlined). In column C the two framework structures are combined within a single cell to make the complete structure of ice IV.

Table 3. Structure factors for ice VI: comparison of calculated (F_c) and observed (F_o) values. Calculated values contain contributions from oxygen atoms only, positions as given in text, temperature parameter $B = 1.5$ Å^2. Observed values from intensities visually measured on precession photographs. Units of electrons per unit cell.

hkl	F_o	F_c	ΔF
200	29.4	−26.8	2.6
400	59.0	60.7	1.7
600	14.2	−13.2	1.0
800	14.7	14.1	0.6
101	7.3	6.4	0.9
201	61.3	59.4	1.9
301	19.2	−20.3	1.1
401	4.5	−3.5	1.0
501	5.3	−5.5	0.2
601	14.6	14.2	0.4
701	10.3	−9.3	1.0
801	4.2	−3.9	0.3
002	34.9	−31.4	3.5
102	54.8	−50.8	4.0
202	19.4	18.9	0.5
302	13.4	15.4	2.0
402	12.0	−14.5	2.5
502	26.7	−28.5	1.8
602	5.7	6.7	1.0
702	<4.4	0.9	
802	4.0	−4.5	0.5
103	32.6	32.7	0.1
203	42.3	−43.5	1.2
303	34.5	−32.0	2.5
403	4.3	3.0	1.3
503	8.1	9.4	1.3
603	12.5	−13.5	1.0
703	15.1	−14.3	0.8
803	4.6	4.0	0.6
004	35.1	34.8	0.3
104	4.1	4.6	0.5
204	8.5	9.2	0.7
304	<4.1	−1.6	
404	17.3	18.2	0.9
504	4.4	3.5	0.9
604	<4.4	−0.6	
704	<3.9	−0.1	
105	17.7	−19.6	1.9
205	14.6	−15.6	1.0
305	21.1	22.9	1.8
405	<4.5	1.2	
505	6.9	−6.9	0.0
605	6.7	−6.5	0.2
006	<4.4	0.3	
106	13.7	13.2	0.5
206	5.0	5.3	0.3
306	4.8	−5.1	0.3
406	<4.4	−0.3	
506	13.6	12.7	0.9
107	<4.4	1.0	
207	12.3	14.4	2.1
307	<4.1	1.4	
407	<3.4	−1.2	
008	13.6	15.9	2.3
108	2.8	2.6	0.2

longer than the hydrogen bonds. Each molecule (both types 2 *a* and 8 *g*) has eight next-nearest neighbors, all at a distance of 3.51 Å. These neighbors represent the closest approach between oxygen atoms of the two separate interpenetrating frameworks.

The special structural feature found here—interpenetration of separately linked frameworks—is a natural way to achieve high density in framework structures based on tetrahedral linkage, in view of the rather open structure that tends to result from such linkage. It is noteworthy that this feature is shown by the highest-pressure forms of ice (VI and VII), but has not yet been reported for high-pressure forms of SiO_2 or for tectosilicate structures.

There is, however, a significant relation between the ice VI structure and certain tectosilicate minerals, the fibrous zeolites. The structures of these minerals (*11*) are based on a tectosilicate chain that is topologically identical with the chain, described above, that occurs in ice VI. The tectosilicate chains are linked together in different ways to form the various different fibrous zeolite structures (*12*). The particular linkage in edingtonite is analogous to what occurs in ice VI (Fig. 4, column B). In edingtonite, however, the chains twist relative to one another in such a way as to collapse the cavities between them and to reduce the equivalent *a*-axial length to about 5.93 Å (compared with 6.27 Å in ice VI). In the zeolite, the collapse of the cavities is governed mainly by interaction between the negatively charged framework and cations (Na^+, Ca^{++}, Ba^{++}) contained in the cavities (*13*); there is also a slight dependence on the water content of the zeolite. In ice VI, the cavities have to be of equal size to the chains, in order to accommodate the second framework; hence there is no collapse. The large openings between pairs of linked chains, which in the zeolite structures allow ion-exchange and dehydration (*13*), are utilized in the ice VI structure for the cross-links between chains of the second framework.

Refinement of the ice VI structure, which is being undertaken with more complete x-ray data now at hand, will permit any slight differences in length among the three types of hydrogen bonds present to be determined, and it may lead to some conclusions about the positions of the hydrogen atoms. This is of interest in relation to the large distortion of bond angles in the ice VI structure, the angle between some of the hydrogen bonds at a given water molecule being as low as 76° and as large as 128°. The detailed study will also, it is hoped, make possible an interpretation of the fact that a very weak but definitely nonzero intensity is observed for the 001 reflection, in violation of the extinction rules for space group $P4_2/nmc$. This reflection suggests the possibility that the orientations of the water molecule become ordered upon cooling to −196°C; it may be possible to determine the nature of this ordering from the x-ray data.

BARCLAY KAMB
Division of Geological Sciences,
California Institute of Technology,
Pasadena 91109

References and Notes

1. S. W. Peterson and H. Levy, *Acta Cryst.* **10**, 70 (1957).
2. G. Honjo and K. Shimaoka, *ibid.*, p. 710; M. Blackman and N. D. Lisgarten, *Advan. Phys.* **7**, 189 (1958).
3. B. Kamb, *Acta Cryst.* **17**, 1437 (1964).
4. ——— and S. K. Datta, *Nature* **187**, 140 (1960).
5. B. Kamb and B. L. Davis, *Proc. Natl. Acad. Sci. U.S.* **52**, 1433 (1964). Structural data for ice VII were obtained at high pressure but in Table 1 are extrapolated to atmospheric pressure by means of data on the quenched form published by Bertie *et al.* (*6*).
6. J. E. Bertie, L. D. Calvert, E. Whalley, *Can. J. Chem.* **42**, 1373 (1964).
7. K. Lonsdale, Ed., *International Tables for X-ray Crystallography* (Kynoch, London, 1959), vol. 1, p. 237.
8. S. Block, C. W. Weir, and G. J. Piermarini, *Science* **148**, 947 (1965).
9. P. W. Bridgman, *Proc. Am. Acad. Arts Sci.* **47**, 441 (1912).
10. L. Pauling, *The Nature of the Chemical Bond* (Cornell Univ. Press, Ithaca, N.Y., 1960), p. 469; J. H. van der Waals and J. C. Patteeuw, *Advan. Chem. Phys.* **2**, 1 (1959).
11. L. Pauling, *Proc. Natl. Acad. Sci. U.S.* **16**, 453 (1930).
12. W. H. Taylor, *Proc. Roy. Soc. London Ser. A* **145**, 80 (1934); W. L. Bragg, *Atomic Structure of Minerals* (Cornell Univ. Press, Ithaca, N.Y., 1937), p. 258.
13. W. M. Meier, *Z. Krist.* **118**, 430 (1960).
14. P. W. Bridgman, *J. Chem. Phys.* **3**, 597 (1935). Density of ice IV is estimated from measured volume difference between D_2O ice IV and ice VI by assuming that the same molar volume difference applies to the H_2O forms, and assuming equal compressibilities for ice IV and VI. The density of ice IV can then be calculated from the known density of ice VI as established crystallographically.
15. P. W. Bridgman, *J. Chem. Phys.* **5**, 964 (1937).
16. M. Blackman and N. D. Lisgarten, *Advan. Phys.* **7**, 197 (1958).
17. J. E. Bertie, L. D. Calvert, and E. Whalley, *J. Chem. Phys.* **38**, 840 (1963).
18. Division of the Geological Sciences, contribution No. 1373. The work was supported by the NSF and the Sloan Foundation. I thank Steven Card and Jon Evans for assistance with the experimental work and calculations, and Linus Pauling for helpful discussion.

20 August 1965